

## Journal Pre-proofs

Electrochemical Synthesis of Carbon-Metal Fluoride Nanocomposites as Cathode Materials for Lithium Batteries

M. Helen, Maximilian Fichtner, M. Anji Reddy

PII: S1388-2481(20)30197-1

DOI: <https://doi.org/10.1016/j.elecom.2020.106846>

Reference: ELECOM 106846

To appear in: *Electrochemistry Communications*

Received Date: 24 August 2020

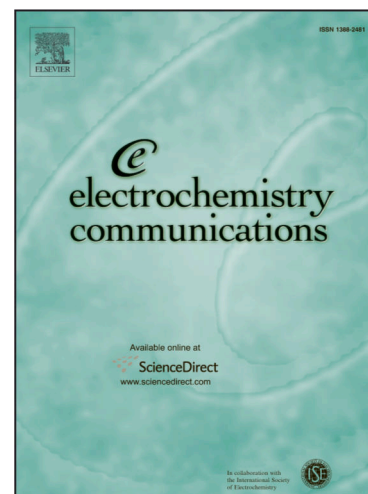
Revised Date: 8 September 2020

Accepted Date: 22 September 2020

Please cite this article as: M. Helen, M. Fichtner, M. Anji Reddy, Electrochemical Synthesis of Carbon-Metal Fluoride Nanocomposites as Cathode Materials for Lithium Batteries, *Electrochemistry Communications* (2020), doi: <https://doi.org/10.1016/j.elecom.2020.106846>

This is a PDF file of an article that has undergone enhancements after acceptance, such as the addition of a cover page and metadata, and formatting for readability, but it is not yet the definitive version of record. This version will undergo additional copyediting, typesetting and review before it is published in its final form, but we are providing this version to give early visibility of the article. Please note that, during the production process, errors may be discovered which could affect the content, and all legal disclaimers that apply to the journal pertain.

© 2020 Published by Elsevier B.V.



## Electrochemical Synthesis of Carbon-Metal Fluoride Nanocomposites as Cathode Materials for Lithium Batteries

M. Helen<sup>a</sup>, Maximilian Fichtner<sup>b,c</sup> and M. Anji Reddy<sup>a,\*</sup>

<sup>a</sup> College of Engineering, Swansea University, Fabian Way, Swansea SA1 8EN, United Kingdom.

<sup>b</sup> Helmholtz Institute Ulm (HIU) Electrochemical Energy Storage, Helmholtzstraße 11, 89081 Ulm, Germany.

<sup>c</sup> Institute of Nanotechnology, Karlsruhe Institute of Technology, P.O. Box 3640, D-76021 Karlsruhe, Germany.

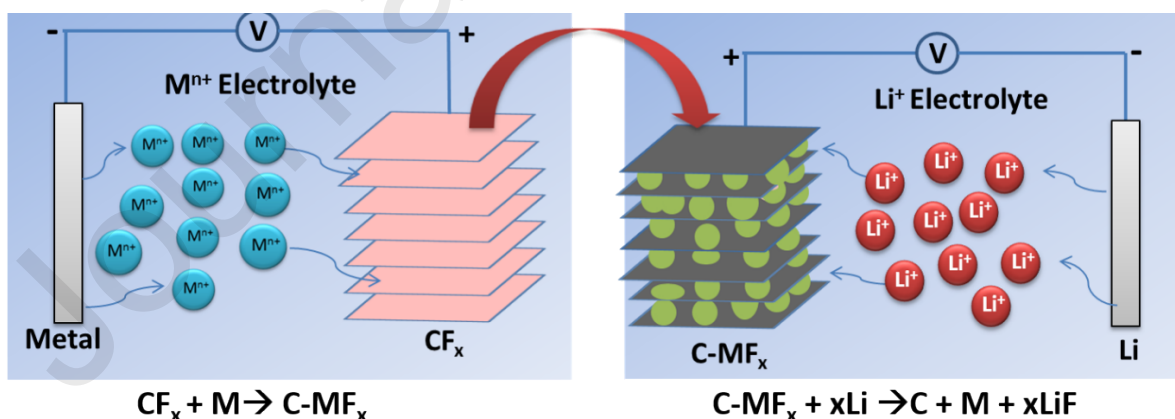
\*Corresponding author Email: [a.r.munnangi@swansea.ac.uk](mailto:a.r.munnangi@swansea.ac.uk)

### Abstract

Herein we have demonstrated an electrochemical method for the synthesis of carbon-metal fluoride nanocomposites (CMNFCs). Electrochemical intercalation of transition metal ions into graphite fluoride ( $CF_x$ ) resulted in the formation of CMNFCs. As a proof-of-concept, we have synthesized C- $FeF_2$  and C- $NiF_2$  nanocomposites by the electrochemical intercalation of  $Fe^{2+}$  and  $Ni^{2+}$  into  $CF_x$  from corresponding non-aqueous electrolytes. The C- $FeF_2$  and C- $NiF_2$  nanocomposites synthesized by this method showed high reversible capacity and cycling stability compared to chemically synthesized analogs as cathode materials for lithium batteries. The reversible capacity of chemically synthesized C- $FeF_2$  is  $181 \text{ mAh g}^{-1}$ , whereas electrochemically synthesized material is  $349 \text{ mAh g}^{-1}$  after 20 cycles. The better cycling performance of electrochemically synthesized C- $FeF_2$  was attributed to the homogeneous distribution of  $FeF_2$  nanoparticles within the carbon matrix enabled by the electrochemical intercalation of  $Fe^{2+}$ . The electrochemical method described here is emission-free, cost-effective, occurs at room temperature, and extendable to the synthesis of several other CMNFCs. Moreover, it might provide new avenues for the synthesis of advanced functional materials.

### Graphical Abstract

A new electrochemical method is demonstrated for the synthesis of carbon-metal fluoride nanocomposites at room temperature.



**Keywords:** CF<sub>x</sub>; metal fluorides; C- $FeF_2$  and C- $NiF_2$ ; lithium batteries.

## Introduction

Metal fluorides are an important class of cathode materials for rechargeable lithium batteries due to their high energy density compared to the conventional insertion-based electrode materials (1-3). However, metal fluorides are electrical insulators and show large volume changes during lithiation and delithiation reactions, which leads to gradual isolation of metal fluoride particles and results in capacity fading. Further, the electrochemical reaction between lithium and conversion-based metal fluorides is slow; therefore, crystallite size of the metal fluorides should be in the nanometer-regime to minimize the reaction path length of metal fluorides with lithium. In a tradeoff, the use of carbon-metal fluoride nanocomposites (CMFNCs) were suggested rather than using pure metal fluorides (4). Indeed, these CMFNCs showed better cycling stability compared to pure metal fluorides (4,5). However, the synthesis of CMFNCs is challenging. Often, mechanical milling was used to synthesize the CMFNCs (6). But the mechanical milling breaks the electronic network of carbon and reduces the total electrical conductivity of the resulting composites. This results in poor cycling stability (6). Alternatively, several chemical methods were suggested for the synthesis of CMFNCs (7-15). Recently we have reported a one-step facile chemical redox method for the synthesis of CMFNCs (16-19). The reaction of  $\text{Fe}(\text{CO})_5$ , with graphite fluoride ( $\text{CF}_x$ ) at 250 °C resulted in the formation of C- $\text{FeF}_2$  nanocomposites (16-19). This method can be applied for the synthesis of various other CMFNCs (C- $\text{CoF}_2$ , C- $\text{MoF}_3$ ) other than C- $\text{FeF}_2$ , by simply changing the metal carbonyl precursor (18). In addition to metal fluorides, we could also synthesize C- $\text{FeO}_x$  and C- $\text{FeS}$  nanocomposites by changing the reactant from  $\text{CF}_x$  to graphite oxide ( $\text{CO}_x$ ) and sulphur-infused ultramicroporous carbon (C- $\text{S}_x$ ) (18). This method produced quality CMFNCs but releases carbon monoxide (CO) as a side product, which is undesirable. Here we report an advanced electrochemical method for the synthesis of CMFNCs. Electrochemical intercalation of  $\text{Fe}^{2+}$  and  $\text{Ni}^{2+}$  into  $\text{CF}_x$  resulted in the electrochemical synthesis of C- $\text{FeF}_2$  and C- $\text{NiF}_2$  nanocomposites, which showed superior electrochemical performance as cathode materials for lithium batteries. The electrochemical method described here do not release any gas (emission-free), occurs at room temperature (RT), cost-effective, and extendable to the synthesis of several other CMFNCs.

## Experimental section

Iron(II) perchlorate hydrate ( $\text{Fe}(\text{ClO}_4)_2 \cdot x\text{H}_2\text{O}$  - 98%), nickel(II) perchlorate hexahydrate ( $\text{Ni}(\text{ClO}_4)_2 \cdot 6\text{H}_2\text{O}$ ),  $\text{CF}_x$ , anhydrous acetonitrile (ACN), and anhydrous tetrahydrofuran (THF) were obtained from Sigma Aldrich. Fe, Ni, and Li foils were obtained from Goodfellow. The Li electrolyte 1.0 M  $\text{LiPF}_6$  in 1:1 ethylene carbonate (EC)/dimethyl carbonate (DMC) (LP30) was obtained from Merck. **Fe and Ni electrolytes were made by dissolving required amounts of perchlorate salts (to prepare 1.0 M electrolytes) in ACN or THF.** Activated molecular sieves (3 Å) were added to these electrolytes to absorb the  $\text{H}_2\text{O}$  molecules present in the perchlorate salts. The carbon content in the  $\text{CF}_x$  sample was estimated by elemental analysis, and the composition was determined as  $\text{CF}_{1.1}$ . Electrode fabrication and assembly of electrochemical cells was done in an argon-filled glove box. The electrodes were fabricated by mixing the active material, acetylene black and polyvinylidene fluoride (PVDF) in the mass ratio of 70:20:10. A slurry containing the above mixture was prepared by using N-methyl-2-pyrrolidinone (NMP), spread on stainless steel (SS) foil (area: 1.13  $\text{cm}^2$ ), and dried on a hot plate at 120 °C for 12 h. Typically, each electrode contained 2-3 mg of the active material ( $\text{CF}_x$ ). **The discharged electrodes collected from the corresponding cells were washed with anhydrous acetonitrile and dried at RT and used further in Li-half cells. The mass loading of  $\text{FeF}_2$  or  $\text{NiF}_2$  was calculated as follows. 1.0 mole of  $\text{CF}_{1.1}$  would react with 0.5 moles of Fe. This results in the formation of  $\text{C}(\text{FeF}_2)_{0.55}$ . The weight percent of  $\text{FeF}_2$  in  $\text{C}(\text{FeF}_2)_{0.55}$  is approximately 80 %. Each electrode contains 2.0 to 3.0 mg of  $\text{CF}_{1.1}$ , which results in the mass loading of 1.6 to 2.4 mg of  $\text{FeF}_2$  in the electrode.** Fe, Ni, and Li foils were used as the negative electrodes in respective cells, and a borosilicate glass fiber sheet saturated with respective electrolyte was used as separator and electrolyte. The cells were placed in an incubator (Binder) to maintain a constant operating temperature of 25 °C. The electrochemical studies were carried out using the Arbin battery cycling unit.

X-ray diffraction (PXRD) patterns were recorded using a Philips X'pert diffractometer equipped with Mo  $K_{\alpha}$  radiation. In the case of  $CF_x$  electrodes, XRD patterns were collected on the electrodes after discharging the electrodes in Fe cells. The discharged  $CF_{1.1}$  electrodes were collected from the corresponding cells washed with anhydrous acetonitrile and dried at RT. Scanning electron microscopy (SEM) was performed with a LEO 1530 at 15 keV using carbon tape as a substrate. Electrochemical studies were performed in Swagelok® type cells. Transmission electron microscopy was carried out on an aberration (image) corrected Titan 80-300 (FEI Company) operated at 80 kV equipped with a Gatan imaging filter Tridiem 863. The material for TEM studies consisted of powder sample free from solvents.

## Results and discussion

$CF_x$  is a primary lithium battery cathode material (20). With an average discharge potential of 2.5 V vs.  $Li^+/Li$  and a theoretical specific capacity of 896 mAh  $g^{-1}$  (by assuming the electrochemical reaction of 1.1 Li),  $CF_x$  is a viable cathode material for primary lithium batteries (Fig. 1a). Though the experimentally observed reduction potential of  $CF_x$  is 2.5 V vs.  $Li^+/Li$ , the thermodynamic reduction potential of  $CF_x$  is 4.21 V vs.  $Li^+/Li$  (21). This high reduction potential of  $CF_x$  makes it thermodynamically feasible for  $Fe^{2+}$  and  $Ni^{2+}$  intercalation. Apart from its high reduction potential,  $CF_x$  also has other advantages as a reactant for the synthesis of CMFNCs.  $CF_x$  is a source of both carbon and fluorine. The insulating  $sp^3$  - hybridized carbon in  $CF_x$  can be reduced to conductive  $sp^2$  carbon upon the deintercalation of fluorine (reduction). Different types of CMFNCs can be synthesized by opting for  $CF_x$  with varying backbones of carbon (19) and further by different carbon to fluorine ratio (17).

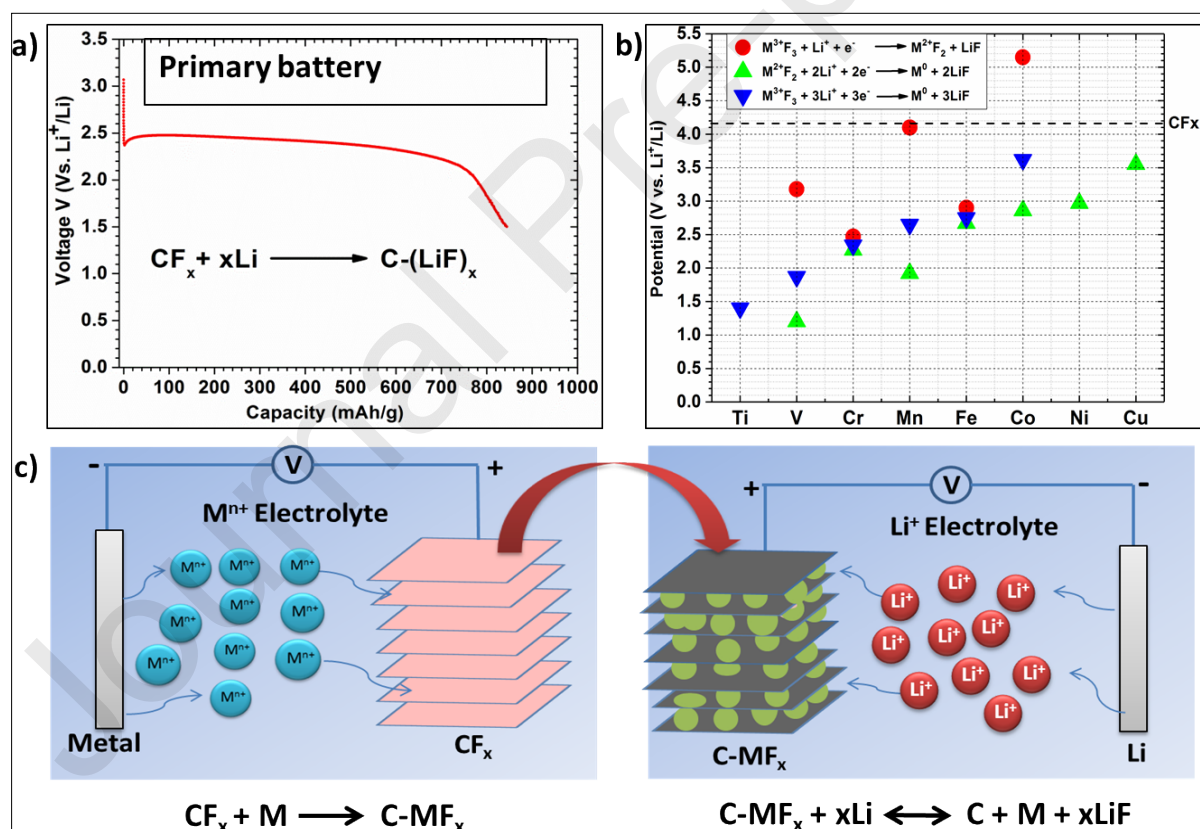


**Figure 1** a) discharge profile of  $CF_x/Li$  cell; b) formation potentials of various metal fluorides and  $CF_{1.1}$  vs.  $Li^+/Li$ ; c) schematic representation of the electrochemical approach used for the synthesis and testing of  $C-FeF_2$  and  $C-NiF_2$  nanocomposites.

The electrochemical reaction of Li with  $CF_x$  results in the formation of LiF crystallites embedded in the carbon matrix. In principle, the process is extendable for the synthesis of transition metal fluorides embedded in a carbon matrix by replacing the Li metal and Li-ion transporting electrolyte with the desired metal and metal-ion transporting electrolyte. Here, we demonstrate such an electrochemical

reaction is indeed extendable to the synthesis of other metal fluorides ( $\text{FeF}_2$  and  $\text{NiF}_2$ ). Lithium exists as a monovalent ( $\text{Li}^+$ ) in the intercalated state. But Fe and Ni can exist in several oxidation states. Therefore, these transition metal ions might have different oxidation states after the intercalation due to the possible internal redox reactions with the host, which highly depends on the host material. In these studies, we assume Fe and Ni are intercalated as  $\text{Fe}^{2+}$  and  $\text{Ni}^{2+}$ , respectively, as they are present as  $\text{Fe}^{2+}$  and  $\text{Ni}^{2+}$  in the respective electrolytes. Fig. 1b compares the formation potentials of various transition metal fluorides and  $\text{CF}_{1.1}$  vs.  $\text{Li}^+/\text{Li}$ . Thermodynamically, it is feasible to synthesize all of the transition metal fluorides beneath the dotted line (Fig. 1b) by reacting  $\text{CF}_x$  with the respective transition metal. The feasibility of such a process depends mainly on two aspects: the reduction of  $\text{CF}_x$  with desired metal should be thermodynamically feasible and on the availability of suitable electrolyte that can transport and deliver the desired metal ions to the intercalation host. Fig. 1c represents the scheme adopted for the electrochemical synthesis of CMFNCs. Using this approach, we have synthesized C- $\text{FeF}_2$  and C- $\text{NiF}_2$  nanocomposites and tested them as cathode materials in rechargeable lithium batteries. **In a typical  $\text{CF}_x/\text{Fe}$  cell, Fe metal will oxidize to  $\text{Fe}^{2+}$  at the anode and dissolves in the electrolyte. For charge balance, the  $\text{Fe}^{2+}$  from the electrolyte will be released to  $\text{CF}_x$  at the cathode. The electrons generated by the oxidation of Fe metal will travel through the external load, reach the cathode, and reduces the  $\text{CF}_x$ . First,  $\text{Fe}^{2+}$  will be desolvated at the surface of  $\text{CF}_x$ . The desolvated  $\text{Fe}^{2+}$  will then be intercalated into the  $\text{CF}_x$  layers. The intercalated  $\text{Fe}^{2+}$  will defluorinate the  $\text{CF}_x$  and nucleate the formation of  $\text{FeF}_2$  particles and conductive carbon. The  $\text{FeF}_2$  particles thus formed will be wrapped in the conductive carbon. Initially, the intercalation reaction is expected to occur at the surface, which then proceeds to bulk.**

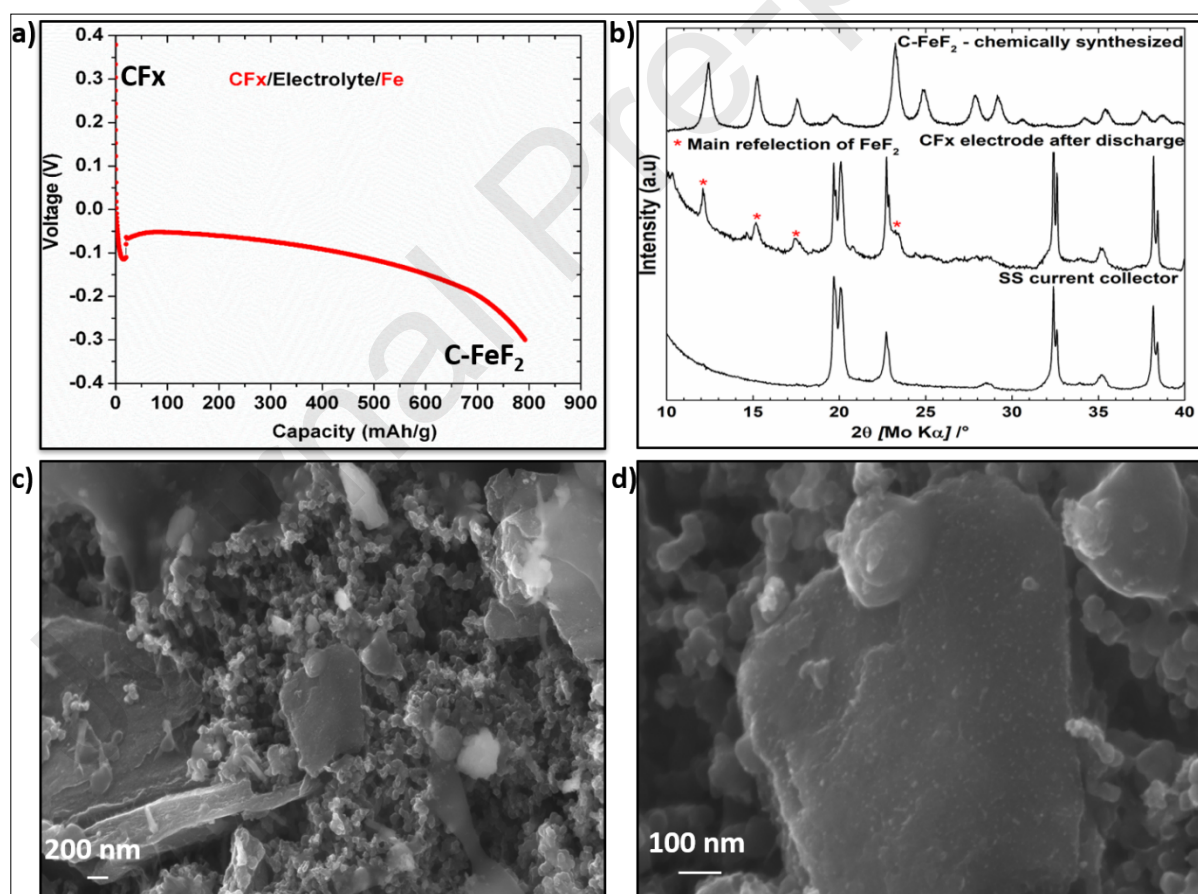


**Figure 2** a) discharge profile of  $\text{CF}_x/\text{Fe}$  cell; b) XRD patterns of stainless steel, electrode obtained after discharging the  $\text{CF}_x/\text{Fe}$  cell down to  $-0.3$  V at  $10$  mA  $\text{g}^{-1}$ , chemically synthesized C- $\text{FeF}_2$ ; c) and d) SEM images of electrochemically synthesized C- $\text{FeF}_2$  nanocomposites at different magnifications.

Electrochemical cells were constructed using  $\text{CF}_x$  as a cathode, iron-metal as the anode, and  $1.0$  M  $\text{Fe}(\text{ClO}_4)_2 \cdot x\text{H}_2\text{O}$  dissolved in acetonitrile as an electrolyte (dried under  $3$  Å molecular sieves before use

to remove the water, which might originate from the dissolved  $\text{Fe}(\text{ClO}_4)_2 \cdot x\text{H}_2\text{O}$ ). Acetonitrile was chosen as a solvent due to its relatively low solvent donor number (DN) of  $14.1 \text{ Kcal mol}^{-1}$ , aprotic nature, and large electrochemical stability window. The low solvent DN means reduced binding energy between the solvent and the cation, which is a prerequisite for the initiation of a desolvation process of metal ions at the surface of the electrode material.

The formation potential of  $\text{CF}_x$  and  $\text{FeF}_2$  is 4.21 and 2.66 V vs.  $\text{Li}^+/\text{Li}$ . The formation potential of  $\text{CF}_x$  against  $\text{Fe}^{2+}/\text{Fe}$  is 1.55 V vs.  $\text{Li}^+/\text{Li}$  (Fig. 1b); hence the formation of  $\text{FeF}_2$  from  $\text{CF}_x$  and iron metal is thermodynamically feasible. Fig. 2a shows the discharge profile of the  $\text{CF}_x/\text{Fe}$  cell. The results of four different  $\text{CF}_x/\text{Fe}$  cells are shown in Fig. S1 (see supporting information). The cells were discharged at a current density of  $10 \text{ mA g}^{-1}$  to  $-0.3 \text{ V}$ . All four cells yield similar discharge profiles with minor differences in the discharge capacity. During the discharge process, the voltage dropped from the open-circuit voltage (OCV) of  $0.4 \text{ V}$  to  $-0.1 \text{ V}$ . Then the voltage was raised to  $-0.05 \text{ V}$ . This small drop and increase of voltage was also seen in  $\text{CF}_x/\text{Li}$  cells (Fig. 1a), and it could be due to the reduced resistance of the electrode due to the nucleation of conductive carbon formed by the reduction of  $\text{CF}_x$ . The average discharge potential of the cell was  $-0.1 \text{ V}$ , which is much lower than the predicted equilibrium potential of  $1.55 \text{ V}$ . The large overpotential observed is consistent with  $\text{CF}_x/\text{Li}$  cells. The average discharge potential of  $\text{CF}_x/\text{Li}$  cell is  $2.5 \text{ V}$ , while the predicted voltage is  $4.21 \text{ V}$ . The large overpotential observed in discharge could be due to the sluggish diffusion of metal cations within the  $\text{CF}_x$  layers. The strong electrostatic force between negatively charged fluoride ions and positively charged cations might impede the diffusion of cations.

We have also tested the discharge behavior of  $\text{CF}_x/\text{Fe}$  cells in  $1.0 \text{ M Fe}(\text{ClO}_4)_2 \cdot x\text{H}_2\text{O}$  dissolved in tetrahydrofuran (THF) as an electrolyte (dried under  $3 \text{ \AA}$  molecular sieves before use). The discharge profiles of two different  $\text{CF}_x/\text{Fe}$  cells tested in THF electrolyte are shown in Fig. S2 (see supporting information). Surprisingly, these cells did not show any significant capacity even when discharged down to  $-1.0 \text{ V}$ . The solvent DN of THF is  $20 \text{ Kcal mol}^{-1}$ . The higher solvent DN of THF (compared to ACN) might lead to the relatively strong binding between THF and  $\text{Fe}^{2+}$  and might not desolvated  $\text{Fe}^{2+}$  at the surface of  $\text{CF}_x$ . These studies might guide in choosing the right solvent for the electrochemical intercalation of transition metal ions.

Fig. 2b compares the XRD patterns of electrochemically synthesized C- $\text{FeF}_2$  with that of chemically synthesized C- $\text{FeF}_2$  nanocomposite (synthesized by reacting  $\text{CF}_x$  and  $\text{Fe}(\text{CO})_5$  at  $250 \text{ }^\circ\text{C}$  (16)). The XRD patterns of electrochemically synthesized C- $\text{FeF}_2$  were directly collected on an electrode coated on stainless steel (SS) current collector. For comparison, the XRD pattern of the SS current collector was incorporated. The reflections marked with \* are the main reflections of  $\text{FeF}_2$  and matches well with the chemically synthesized  $\text{FeF}_2$ . The other strong reflections were due to the SS current collector. The XRD results provide direct evidence for the formation of  $\text{FeF}_2$ . Fig. 2c, d shows the SEM images of C- $\text{FeF}_2$  electrodes with different magnifications. Two different morphologies are evident from the SEM images. The bigger platelet-like particles are C- $\text{FeF}_2$ , and the smaller spherical particles are conductive carbon used in the fabrication of the electrodes. No  $\text{FeF}_2$  particles were seen on the surface of the platelets and confirm the confinement of  $\text{FeF}_2$  within the carbon matrix. **Fig. S3 shows the energy-dispersive X-ray (EDX) images of C- $\text{FeF}_2$  nanocomposites. From the elemental mapping, it is evident that Fe, F, and C were distributed uniformly. Fig. S4 shows the transmission electron microscopy (TEM) image and selective area electron diffraction (SAED) pattern of C- $\text{FeF}_2$  nanocomposites. TEM reveals the presence of nanocrystalline  $\text{FeF}_2$  (5 to 10 nm in size) particles embedded uniformly in the carbon matrix. The dotted ED patterns further indicate the crystallinity of  $\text{FeF}_2$  nanoparticles.** For comparison, SEM images of pure  $\text{CF}_x$  (Fig. S5b) and chemically synthesized C- $\text{FeF}_2$  nanocomposites (Fig. S6) are given in supporting information. The morphologies of electrochemically synthesized and chemically synthesized nanocomposites appear to be similar.

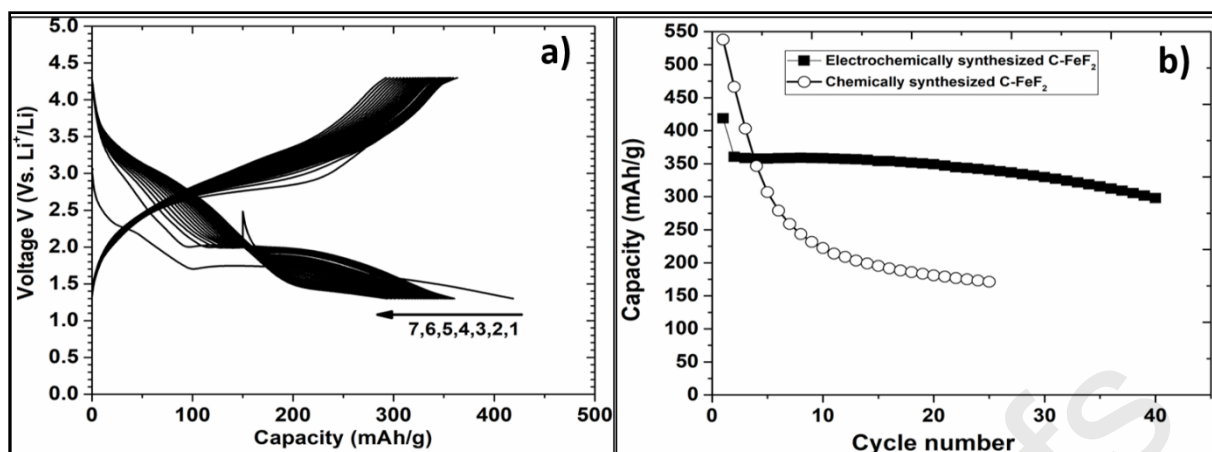


**Figure 3** a) shows the discharge-charge profiles of C-FeF<sub>2</sub> electrode obtained after discharging the CF<sub>x</sub>/Fe cell, b) it's cycling behavior (the cycling behavior of chemically synthesized C-FeF<sub>2</sub> is included for comparison). The cells were cycled at 20 mA g<sup>-1</sup>. Capacities are with respect to the active material FeF<sub>2</sub> weight in the composite.

From the above results and discussion, it is apparent that the formation of FeF<sub>2</sub> nanoparticles is a result of the intercalation of Fe<sup>2+</sup> into CF<sub>x</sub> layers. However, it could be hypothesized that the formation of FeF<sub>2</sub> nanoparticles is due to the surface reaction between CF<sub>x</sub> and Fe<sup>2+</sup>. From the discharge capacity of the CF<sub>x</sub>/Fe cell (more than 800 mAh g<sup>-1</sup>), it is clear that the full amount of CF<sub>x</sub> is reacted. The surface reaction between CF<sub>x</sub> and Fe<sup>2+</sup> cannot explain the high capacity observed in CF<sub>x</sub>/Fe cell. Further, from the SEM and TEM images, it is clear that the FeF<sub>2</sub> nanoparticles were well embedded in the carbon matrix. This indicates the reaction between Fe<sup>2+</sup> and F<sup>-</sup> occurred in the bulk of the CF<sub>x</sub>. If there is a significant reaction at the surface, a large amount of FeF<sub>2</sub> particles would have formed on the surface. Further, to assume a surface reaction between F<sup>-</sup> and Fe<sup>2+</sup>, F<sup>-</sup> should move to the surface of the CF<sub>x</sub>. The carbon-fluorine bond in CF<sub>x</sub> is covalent. Therefore, it is unlikely that F<sup>-</sup> would move to the CF<sub>x</sub> surface at RT. It is more likely that Fe<sup>2+</sup> intercalated into CF<sub>x</sub> layers and resulted in the formation of FeF<sub>2</sub>.

Fig. 3a and b show the discharge-charge profiles of the C-FeF<sub>2</sub> electrode and its cycling behavior. The cells were cycled at 20 mA g<sup>-1</sup>. The capacities were calculated with respect to the active material weight (FeF<sub>2</sub>). The first discharge and charge capacities of the cell were 418 mAh g<sup>-1</sup>, and 363 mAh g<sup>-1</sup> with an irreversible capacity loss (ICL) of 55 mAh g<sup>-1</sup>. The cells show a stable reversible capacity up to 15 cycles (353 mAh g<sup>-1</sup>) and faded rather quickly to 297 mAh g<sup>-1</sup> after 40 cycles. Interestingly, the cycling performance of the electrochemically synthesized C-FeF<sub>2</sub> shows better stability than chemically synthesized C-FeF<sub>2</sub> (synthesized by reacting CF<sub>x</sub> and Fe(CO)<sub>5</sub> at 250 °C (16)). The reversible capacity of chemically synthesized C-FeF<sub>2</sub> is 181 mAh g<sup>-1</sup>, whereas electrochemically synthesized material is 349 mAh g<sup>-1</sup> after 20 cycles. The theoretical specific capacity of FeF<sub>2</sub> is 571 mAh g<sup>-1</sup>. However, we observed only 418 mAh g<sup>-1</sup> in the first discharge. The low discharge capacity of electrochemically synthesized C-FeF<sub>2</sub> might be due to the leaching out of some FeF<sub>2</sub> particles from the electrode during the washing process of the electrode. Washing was performed with anhydrous acetonitrile to remove the electrolyte impurities from the CF<sub>x</sub>/Fe cell.

The better cycling performance of electrochemically synthesized C-FeF<sub>2</sub> compared to chemically synthesized nanocomposites might be due to the homogeneous distribution of FeF<sub>2</sub> nanoparticles in the carbon matrix in the electrochemical method. In the chemical method, CF<sub>x</sub> and Fe(CO)<sub>5</sub> were gradually heated in a closed Swagelok cell reactor at 250 °C for 24h. In this reaction, initially, Fe(CO)<sub>5</sub> vaporizes at 105 °C (Fe(CO)<sub>5</sub> gas will insert into CF<sub>x</sub> layers under autogenous pressure), decomposes at 150 °C, and produces the iron nanoparticles. The iron nanoparticles will reduce the CF<sub>x</sub> and form FeF<sub>2</sub> and conductive carbon at 250 °C (16,17). These FeF<sub>2</sub> nanoparticles will be wrapped in carbon. As the final reaction occurs at 250 °C, there will be a certain amount of agglomeration of FeF<sub>2</sub> particles within the carbon matrix. In contrast to the chemical method, the electrochemical process occurs at RT and

low current rates ( $10 \text{ mA g}^{-1}$ ). The kinetic energy available for the agglomeration of the  $\text{FeF}_2$  particles is relatively low in this case and should allow better dispersion of  $\text{FeF}_2$  crystallites within the carbon matrix. Therefore, the electrochemical method provided better control over the reaction and resulted in a suitable product for electrochemical applications. Homogeneous distribution of  $\text{FeF}_2$  nanoparticles can better accommodate the volume changes that occur in the  $\text{FeF}_2$  during discharge-charge reactions and reduces capacity fading.

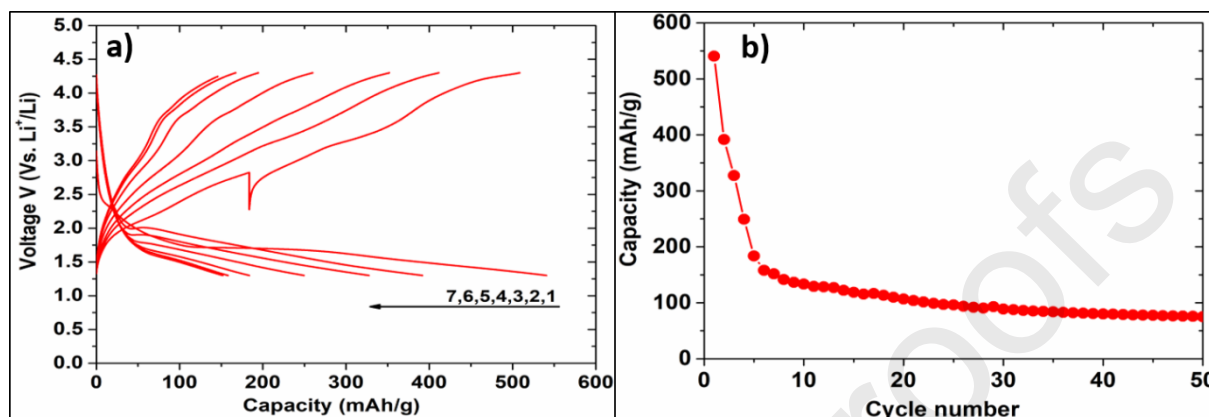


**Figure 4** a) shows the discharge-charge profiles of C-NiF<sub>2</sub> electrode obtained after discharging the CF<sub>x</sub>/Ni cell, b) its cycling behavior. The cells were cycled at  $20 \text{ mA g}^{-1}$ . Capacities are with respect to the active material NiF<sub>2</sub> weight in the composite.

To further validate this electrochemical method, we have synthesized C-NiF<sub>2</sub> nanocomposites similar to C-FeF<sub>2</sub> nanocomposites from CF<sub>x</sub>. **Fig. S7** shows the discharge profile of the CF<sub>x</sub>/Ni cell obtained in 1.0 M Ni(ClO<sub>4</sub>)<sub>2</sub> acetonitrile electrolyte. The average discharge potential of the CF<sub>x</sub>/Ni cell is -0.3 V, 0.2 V less compared to that of CF<sub>x</sub>/Fe cell. The low discharge potential of CF<sub>x</sub>/Ni cell is due to the high reduction potential of NiF<sub>2</sub> compared to FeF<sub>2</sub> (Fig. 1b). The reduction potential of FeF<sub>2</sub> is 2.66, and NiF<sub>2</sub> is 2.94 V vs. Li<sup>+</sup>/Li. This results in a low overall reduction potential of Ni/CF<sub>x</sub> cells. Fig. 4a and b show the discharge-charge profiles of the C-NiF<sub>2</sub> electrode and its cycling behavior. In the case of C-NiF<sub>2</sub>, the first discharge capacity was  $540 \text{ mAh g}^{-1}$ , close to the theoretical specific capacity of  $554 \text{ mAh g}^{-1}$  (Fig. 4a). However, in the case of C-NiF<sub>2</sub> capacity faded rapidly with cycling and reached a reversible capacity of  $75 \text{ mAh g}^{-1}$  after 50 cycles (Fig. 4b). We have not synthesized C-NiF<sub>2</sub> nanocomposite by the chemical method using nickel carbonyl and CF<sub>x</sub> due to the high toxicity of nickel tetracarbonyl (Ni(CO)<sub>4</sub>). Therefore, we could not directly compare the cycling performance of electrochemically synthesized C-NiF<sub>2</sub> and chemically synthesized sample. Nevertheless, the electrochemically synthesized C-NiF<sub>2</sub> nanocomposites showed better cycling stability compared to the chemically synthesized multiwalled carbon nanotube - NiF<sub>2</sub> nanocomposites reported by other authors (22).

## Conclusions

We have demonstrated a new electrochemical method for the synthesis of carbon-metal fluoride nanocomposites. Electrochemical intercalation of Fe<sup>2+</sup> and Ni<sup>2+</sup> into CF<sub>x</sub> led to the formation of C-FeF<sub>2</sub> and C-NiF<sub>2</sub> nanocomposites, which showed better electrochemical performance compared to the chemically synthesized C-MF<sub>2</sub> nanocomposites as cathode materials for lithium batteries. The electrochemical method described here is environmentally benign, cost-effective, occurs at RT, and extendable to synthesize several other CMFNCs and possibly to the electrochemical synthesis of carbon-metal oxides and carbon-metal sulphide nanocomposites. Such studies are under progress.

## Supporting information (SI)

Supporting information is available on electrochemical results on CF<sub>x</sub>/Fe and CF<sub>x</sub>/Ni cells, XRD, SEM, TEM, and EDX of electrochemically synthesized C-FeF<sub>2</sub> nanocomposites. XRD and SEM of CF<sub>x</sub>. SEM image of chemically synthesized C-FeF<sub>2</sub> nanocomposites.



## Acknowledgments

We thank and acknowledge Dr. V. S. K. Chakravadhanula for providing TEM images and Karlsruhe Nano Micro Facility (KNMF) for providing access to TEM facility. This work contributes to the research performed at CELEST (Center for Electrochemical Energy Storage Ulm-Karlsruhe). MF acknowledges partial funding by the German Research Foundation (DFG) under Project ID 390874152 (POLiS Cluster of Excellence).

## Reference

1. G. G. Amatucci and N. Pereira, *J. Fluorine Chem.*, 2007, 128, 243–262.
2. J. Cabana, L. Monconduit, D. Larcher and M. R. Palacin, *Adv. Mater.*, 2010, 22, E170–E192.
3. D. Andre, S. J. Kim, P. Lamp, S. F. Lux, F. Maglia, O. Paschosa and B. Stiaszny, *J. Mater. Chem. A*, 2015, 3, 6709–6732.
4. F. Badway, N. Pereira, F. Cosandey and G. G. Amatucci, *J. Electrochem. Soc.*, 2003, 150, A1209–A1218.
5. N. Pereira, F. Badway, M. Wartelsky, S. Gunn and G. G. Amatucci, *J. Electrochem. Soc.*, 2009, 156, A407–A416.
6. I. Plitz, F. Badway, J. Al-Sharab, A. Du Pasquier, F. Cosandey and G. G. Amatucci, *J. Electrochem. Soc.*, 2005, 152, A307–A315.
7. T. Li, L. Li, Y. L. Cao, X. P. Ai and H. X. Yang, *J. Phys. Chem. C*, 2010, 114, 3190–3195.
8. L. Li, F. Meng and S. Jin, *Nano Lett.*, 2012, 12, 6030–6037.
9. C. Li, L. Gu, S. Tsukimoto, P. A. van Aken and J. Maier, *Adv. Mater.*, 2010, 22, 3650–3654.
10. K. Rui, Z. Wen, Y. Lu, J. Jin and C. Shen, *Adv. Energy Mater.*, 2015, 5, 1401716.
11. Y. Lu, Z. Wen, J. Jin, X. Wu and K. Rui, *Chem. Commun.*, 2014, 50, 6487–6490.
12. Y. Lu, Z. Wen, J. Jin, K. Rui and X. Wu, *Phys. Chem. Chem. Phys.*, 2014, 16, 8556–8562.
13. R. Prakash, A. K. Mishra, A. Roth, Ch. Kübel, T. Scherer, M. Ghafari, H. Hahn and M. Fichtner, *J. Mater. Chem.*, 2010, 20, 1871–1876.
14. C. Wall, R. Prakash, C. Kübel, H. Hahn and M. Fichtner, *J. Alloys Compd.*, 2012, 530, 121–126.
15. F. Wu, V. Srot, S. Chen, S. Lorgner, P. A. van Aken, J. Maier, Y. Yu, *Adv. Mater.* 2019, 31, 1905146.
16. M. Anji Reddy, B. Breitung, V.S.K. Chakravadhanula, C. Wall, M. Engel, C. Kübel, A. K. Powell, H. Hahn and M. Fichtner, *Adv. Energy Mater.* 2013, 3, 308–313.
17. B. Breitung, M. Anji Reddy, V. S. K. Chakravadhanula, M. Engel, C. Kübel, A. K. Powell, H. Hahn, M. Fichtner, *Beilstein J. Nanotechnol.* 2013, 4, 705–713.
18. M. Anji Reddy, B. Breitung, C. Wall, S. Trivedi, V. S. K. Chakravadhanula, M. Helen and M. Fichtner, *Energy Technol.* 2016, 4, 201–211.
19. M. Anji Reddy, B. Breitung, V. S. K. Chakravadhanula, M. Helen, R. Witte, C. Rongeat, C. Kübel, H. Hahn and M. Fichtner, *RSC Adv.*, 2018, 8, 36802–36811.
20. M. Anji Reddy, B. Breitung, and M. Fichtner, *ACS Appl. Mater. Interfaces*, 2013, 5, 11207–11211.
21. J. L. Wood, R. B. Badachhape, R. J. Lagow, J. L. Margrave, *J. Phys. Chem.* 1969, 73, 3139–3142.
22. Q. Huang, T.P. Pollard, X. Ren, D. Kim, A. Magasinski, O. Borodin, and G. Yushin, *Small* 2019, 15, 1804670–1804681.

## Credit Author Statement:

**Author Contributions:** M.A.R. conceived the idea for the project. M.A.R. and M.H. designed and performed the experiments. M.A.R., M.H. and M.F discussed the results, correlated the data and wrote the manuscript.

## Highlights

- A new electrochemical method is demonstrated for the synthesis of carbon-metal fluoride nanocomposites at room temperature.
- Electrochemical intercalation of transition metal ions into graphite fluoride from non-aqueous electrolytes
- Synthesis of C-FeF<sub>2</sub> and C-NiF<sub>2</sub> nanocomposites room temperature by the electrochemical intercalation of Fe<sup>2+</sup> and Ni<sup>2+</sup> into CF<sub>x</sub>
- Emission-free, cost-effective, room-temperature, method for the synthesis of carbon-metal fluoride nanocomposites and other advanced functional materials.

Journal Pre-proofs